Kinetics of Carbonization and Graphitization of PBO Fiber

JAMES A. NEWELL,[1,*] DAN D. EDIE,[2] and E. LOREN FULLER, JR.[3]

[1]Department of Chemical Engineering, University of North Dakota, Grand Forks, North Dakota 58202-7101, [2]Department of Chemical Engineering and Center for Advanced Engineering Fibers, Clemson University, Clemson, South Carolina 29634-0909, and [3]Metals and Ceramics Division, Oak Ridge National Laboratory, Oak Ridge, Tennessee 37831

SYNOPSIS

PBO [poly(*p*-phenylenebenzobisoxazole)] fiber has been shown to convert to an ordered carbon fiber without the need for stabilization. This article presents the first detailed analysis of the carbonization and graphitization behavior of this unique material. The carbonization process was modeled as a series of free-radical reactions, and thermogravimetric analysis was used to determine an activation energy of 76 ± 6 kcal/mol for the thermal initiation of free radicals. The initiation reaction data then were applied to determine the temperature dependence of the termination reaction. Additionally, the development of long-range order in the graphitizing fiber was examined. The spacing between graphene planes was shown to decrease with increasing treatment temperature and soak duration. Carbonized PBO fibers developed more long-range order than carbon fibers produced from other polymers, which may partially explain why these PBO-based fibers display excellent lattice-dependent properties. Finally, an Arrhenius analysis found the activation energy for graphitization to be 120 ± 17 kcal/mol. © 1996 John Wiley & Sons, Inc.

INTRODUCTION

High-performance composites are exceptionally light and exhibit mechanical properties superior to conventional metals. Because these advanced composites consist of more than 50% fiber by volume,[1] considerable research has been directed toward enhancing the properties of these fibers. Nevertheless, significant deficiencies remain in all reinforcing fibers.

Fibers with moderate strength have been produced from polymers such as nylon for over 50 years. However, recently a new generation of advanced polymeric fibers with improved mechanical properties has been developed. Because of their rigid-rod aromatic backbones, this new variety of polymer tends to exhibit liquid crystalline behavior.[2] Some of these liquid crystalline polymers can be solution spun to produce highly oriented fibers with tensile moduli approaching 90% of the theoretical limit.[3] Examples of these high-performance polymers include Kevlar [poly(*p*-phenylene terepthalamide)], PBZT [poly(*p*-phenylene benzobisthiazole)], and PBO [poly(*p*-phenylene benzobisoxazole)] shown in Figure 1.

While these polymers exhibit exceptional tensile properties, their compressive strengths are dramatically inferior to those of most carbon fibers. Unfortunately, this deficiency in compressive strength severely limits the applicability of high-performance polymeric fibers and their composites. Tensile and compressive properties for typical commercial high-performance polymeric and carbon fibers are presented in Table I.[4]

Carbon fibers offer an alternative to high-performance polymeric fibers. Carbon fibers are superior in stiffness to all high-performance polymer fibers and still possess exceptional tensile strengths.[1] Additionally, carbon fibers have the advantage of exceptional thermal properties. Some carbon fibers produced from petroleum pitch precursors have thermal conductivities 3 times greater than copper.[5] Most importantly, the compressive strengths of nearly all carbon fibers are substantially better than

* To whom correspondence should be addressed.

Journal of Applied Polymer Science, Vol. 60, 825–832 (1996)
 CCC 0021-8995/96/060825-08

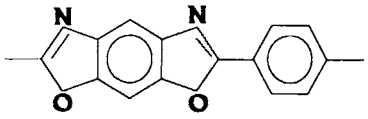

Figure 1 The repeat unit of PBO.

those of the best polymeric fibers. However, the use of carbon fibers is limited by their high cost.[6] This high cost results from the cost of the precursor and the cumbersome, energy-intensive process required to convert the precursor to carbon fiber.

The limiting step in production is the need for a lengthy period of oxidative stabilization prior to the carbonization of the material. This stabilization is necessary to convert the material into a thermally stable form that is able to withstand the extreme temperatures of carbonization without melting or losing molecular orientation. Therefore, a material requiring no stabilization prior to carbonizing would be highly desirable.

Nearly all commercial carbon fibers are produced from either pitch or polyacrylonitrile (PAN). Both pitch and PAN require stabilization prior to carbonization. Advanced polymeric fibers, PBO in particular, offer several distinct advantages over these traditional precursor materials. The presence of aromatic rings in the main chain backbone causes these high-performance polymers to exhibit greater rigidity than polymers with flexible alkane backbones. When processed into fiber form, the rigid-rod structure of these new polymers provides a high degree of axial orientation that may facilitate the process of carbonization. Further, the large proportion of aromatic carbons in the precursor material makes a high carbon yield more likely. Additionally the exceptional crystallinity of PBO enables the unstabilized fiber to withstand the extreme temperatures of carbonization without melting. The superior tensile properties displayed by PBO combined with its extreme axial orientation, its high aromatic carbon content, and the presence of oxygen in the main polymer chain make PBO an ideal candidate for conversion to carbon fiber.

More importantly, it was shown that PBO can be converted directly to an ordered carbon fiber without the need for stabilization.[7] Previous studies[8] have explored the effects of processing conditions on the properties of the resultant PBO-based carbon fibers. However, it is essential to develop a more detailed understanding of the conversion of the polymer into a carbon fiber and to characterize the development of 3-dimensional crystalline order within the carbonized fiber.

It is generally accepted that carbonization is essentially a thermal polymerization process.[9] The chemical and physical changes associated with carbonization include an increase in molecular weight,[10] a decrease in solubility,[11] an increase in carbon to hydrogen ratio,[9] an increase in the size of aromatic layers,[12] and an increase in the free-radical concentration.[13] All of these changes are consistent with a free-radical polymerization process.

Crosslinks between molecules must form during carbonization to prevent melting and volatilization at high temperatures. Throughout the carbonization process, small fragments break off from the polymer chain and are lost as gases. The remaining molecular fragments condense, increasing the aromatic content of the material.[14]

Although there is general agreement that carbonization is a free-radical polymerization process, little attention has been given to the actual chemical kinetics involved. In fact, much of the reported carbonization "kinetics" have really been either crystal growth rates more properly associated with graphitization, or the time-dependent evolution of a given structural parameter.

Another dilemma limiting the availability of kinetic data results from the complexity of free-radical reactions. A free-radical process can be broken into three distinct stages: initiation, propagation, and termination. Each of these reactions must be considered separately. The initiation reaction is the most straightforward to characterize. Here, the stable material must initiate free radicals that, in turn, initiate the reaction. The initiation could involve use of light, heat, radiation, or chemical initiators. Almost invariably, the initiation process requires the breaking of a stable chemical bond. Therefore, this step is relatively slow and measurable. However, the probabilistic nature of free-radical reactions makes it quite difficult to accurately determine even the activation energy of the initiation reaction. Because

Table I Tensile and Compressive Properties of Commercial High-Performance Fibers[4]

Material	Tensile Strength (GPa)	Tensile Modulus (GPa)	Compressive Strength (GPa)
Kevlar 49	3.5	125	0.39–0.49
Kevlar 149	3.4	185	0.32–0.46
PBT	4.1	325	0.26–0.41
PBO	5.7	360	0.20–0.40
TORAY M60J carbon fiber	3.8	585	1.67

of this, most activation energies for even simple free-radical reactions are accurate to only ±0.5 kcal/mol.[15]

The propagation reaction is even more difficult to characterize. Free radicals are inherently unstable. Therefore, each radical exists for extremely short periods of time before reacting again. Thus, most agree that the rate of the propagation reaction is orders of magnitude faster than the rate of the initiation reaction that precedes it.[15] Thus, the direct quantitative analysis of propagation rates is virtually impossible.

The termination reaction is also difficult to characterize directly. When two unstable radicals meet, they combine to terminate the radicalization process. Because the radical species are highly unstable, the activation energy of the termination reaction is much smaller than that of the initiation reaction. In fact, the activation energy of the termination reaction is generally taken to be zero.[16]

Unless the specific concentrations of unreacted reactant and converted product can be measured accurately, the termination rate cannot be determined directly. However, some information regarding the character of the termination reaction can be obtained through thermogravimetric analysis (TGA).

THEORETICAL DEVELOPMENT

Carbonization Kinetics

In the current study, the free-radical reactions associated with the carbonization of PBO were modeled as a series of three reactions:

$$P \rightarrow R^{\bullet} \quad \text{(initiation)}$$

$$R^{\bullet} + P \rightarrow R^{\bullet} \quad \text{(propagation)}$$

$$R^{\bullet} + R^{\bullet} \rightarrow C \quad \text{(termination)}$$

where P is a PBO molecule, $R^{\bullet}$ is a free-radical containing a molecular fragment, and C is a carbonized molecule.

The initiation reaction is induced by the thermal energy associated with carbonization temperatures. This energy strains the bonds between the atoms comprising the PBO molecule. The only bonds in the entire polymer backbone that are not stabilized by π bonding are the carbon–oxygen and the carbon–nitrogen bonds between the bisoxazole rings and the phenylene carbons. The carbon–nitrogen σ bond is the weaker of these bonds. In addition to the adjacent benzene ring that helps stabilize the free radical formed by the breakage of this bond, the nitrogen is double bonded to the carbon in the oxazole ring. This also provides greater stability for the initial free radical.

Determining the appropriate kinetic constants for the proposed initiation reaction is relatively straightforward. Because no external initiator is needed and the monomer pool is essentially infinite, the initiation reaction can be assumed to be of zero order. Thus,

$$\nu_I = k_I \tag{1}$$

where ν_I is the rate of the initiation reaction and k_I is the zero-order rate constant. Application of the Arrhenius equation allows eq. (1) to be written as

$$\nu_I = k_{IO}\exp\left(-\frac{E_A}{RT}\right) \tag{2}$$

where k_{IO} is the preexponential Arrhenius constant, E_A is the activation energy of the initiation reaction, R is the gas constant, and T is absolute temperature. The termination reaction can be represented by

$$\nu_T = k_T[R^{\bullet}]^2 \tag{3}$$

An overall free-radical balance provides

$$\frac{d[R^{\bullet}]}{dt} = k_{IO}\exp\left(-\frac{E_A}{RT}\right) - k_T[R^{\bullet}]^2 \tag{4}$$

However, the unstable nature of free radicals makes the activation energy for termination very small and, in fact, the energy is generally assumed to be zero.[9] Thus, the termination rate constant has no temperature dependence.

The transient nature of free radicals prevents $[R^{\bullet}]$ from being measured directly. However, some boundary approximations can be made. At the onset of initiation, the concentration of free radicals is small, so it can be assumed that the rate of initiation is much greater than the termination rate. Thus, a plot of $d[R^{\bullet}]/dt$ versus T^{-1} would provide both the activation energy and the preexponential Arrhenius constant. The model assumes that the initiation rate of free radicals is directly proportional to the observed mass loss during heating. If free-radical reactions serve as the primary mechanism of mass release, it is reasonable to assume that an increase in free radicals would lead to a proportional increase in mass loss. Therefore, at initial times, eq. (4) could be approximated by

$$K\frac{dM}{dt} = k_{IO}\exp\left(-\frac{E_A}{RT}\right) \quad (5)$$

where M is the sample mass and K is a proportionality constant. Initial mass loss data may be obtained from isothermal TGA trials at different temperatures.

If the termination reaction remained insignificant, the Arrhenius relationship would hold throughout the entire region of mass loss. However, as temperature increases and more free radicals form, the termination reaction becomes increasingly significant, and the complete form of eq. (4) applies.

$$\frac{dM}{dt} \approx \frac{1}{K}\frac{d[R^{\cdot}]}{dt} = \frac{k_{IO}}{K}\exp\left(-\frac{E_A}{RT}\right) - \frac{k_T}{K}[R^{\cdot}]^2 \quad (6)$$

or, alternatively,

$$\nu_T = \frac{k_{IO}}{K}\exp\left(-\frac{E_A}{RT}\right) - \frac{dM}{dt} \quad (7)$$

If eq. (7) is valid, then the behavior of a ramped TGA trial can be predicted from the data obtained in the isothermal trials. In the early stages of mass loss, the initiation reaction should dominate, thus the termination rate should be very small. As temperature increases, the free radical concentration must increase and the termination reaction should become increasingly significant. Also, because temperature is a linear function of time in the ramped trial, the dt in eq. (7) can be replaced by $(1/\alpha)dT$, where α is the linear heating rate. Thus, the right side of eq. (7) can be written as a function of temperature only.

Graphitization Kinetics

At temperatures above 1600°C, carbonized PBO fibers begin to develop some long-range order. Initially, these fibers consist of highly disordered or turbostratic sheets of aromatic molecules. Eventually, relatively ordered graphene planes develop within the fibers. In the ideal case, these fibers would ultimately have a crystal structure identical to graphite, as pictured in Figure 2. The average distance between the graphene layer planes (d_{002}) provides one measure of the order within the fiber. As the fiber becomes more ordered, the mean d spacing should become closer to the 3.35 Å associated with graphite, and the size of the ordered region, or the stack height (L_c) should increase.

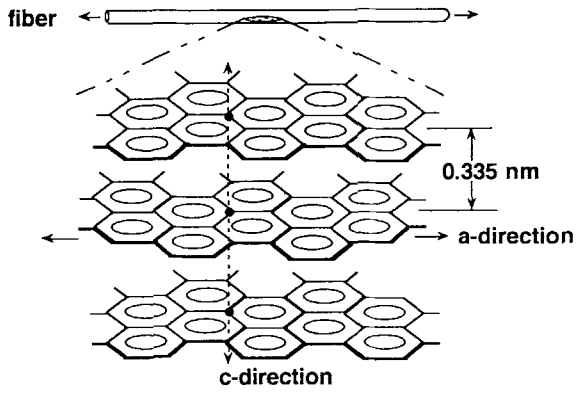

Figure 2 The ideal graphitic fiber.

Crystallite growth is a kinetic phenomenon. The crystallite growth can be represented by the classical Arrhenius kinetic equation of the form

$$\frac{dL_c}{dt} = k_0\exp\left(-\frac{E'_A}{RT}\right) \quad (8)$$

where L_c is the crystallite size of stack height, dt is the change in time, k_0 is the preexponential kinetic constant, E'_A is the activation energy of the graphitization process, R is the gas constant in appropriate units, and T is the absolute temperature of the heat treatment.[17] Equation (8) can be rewritten as

$$\ln\left(\frac{dL_c}{dt}\right) = \ln(k_0) - \frac{E'_A}{RT} \quad (9)$$

In this form, the activation energy and preexponential constant can be determined readily from a plot of $\ln(dL_c/dt)$ versus $1/T$.

EXPERIMENTAL

The PBO fiber used in this study was supplied by the Dow Chemical Company. This fiber was produced using the process described by Ledbetter et al.,[18] and the average filament diameter was 11.6 ± 0.2 μm. The carbonization kinetics of PBO fiber were examined through a series of TGA experiments, while the graphitization kinetics were examined using wide angle X-ray diffraction.

Carbonization Studies

TGA trials were performed in two different modes, ramped and isothermal. In the ramped mode, approximately 2 mg of unstabilized PBO fibers were

placed in the platinum balance pan of a Dupont model 951 TGA system. The fiber samples were heated under industrial grade argon at a linear rate of 10°C/min from ambient temperature to 800°C. Temperature, time, and mass data were recorded at 0.1-s intervals by a TA2100 data compilation system.

In the isothermal mode, the TGA system was heated to the desired temperature before the fibers were placed in the heated zone. Once the system reached the set-point temperature, the balance plan was slid into the hot zone. Within seconds, the temperature of the fibers reached the hot zone temperature. The system was maintained at a constant temperature for the remainder of the experiment.

Analysis of off gases was performed on a UTI model 100C precision gas analyzer. Spectral analysis was performed by a Spectralink software package on a Hewlett–Packard Vectra 286 personal computer. The mass spectrometer was connected to a Mettler recording vacuum thermoanalyzer. Approximately 30 mg of PBO fiber were loaded onto the balance. The system was sealed and placed under vacuum for 30 min. Helium was then passed through the sample chamber. Emissions from the sample chamber were monitored continuously by the mass spectrometer and background gas levels were permitted to equilibrate before heating was initiated.

The PBO samples were heated at a linear rate of 10°C/min to a temperature of 1400°C. Temperature and mass data were continuously recorded by the Mettler system and the effluent gas was sent directly to the sample port of the mass spectrometer. All spectra were subjected to background correction, although the unique pumping system of the mass spectrometer minimized the background gases. Fomblin oil, a synthetic perfluoropolyether compound, was used for lubrication because it made virtually no contribution to the background scatter. Thirteen peaks were monitored throughout the experimental trials. These peaks corresponded to molecular weights of 2, 12, 14, 15, 16, 17, 18, 27, 28, 30, 32, 44, and 46. Spectral scans were performed every 20 s.

Graphitization Studies

Unstabilized PBO fibers were cut into 6-in. lengths and placed in the hearth of a graphite resistance furnace. The furnace temperature was measured by a Raytec pyrometer, which also served as an input to a Northrup Electromax programmable controller. After placing the fiber sample in the hearth, the furnace was sealed and a series of evacuation cycles in which the furnace is subjected to vacuum, then filled with helium, was performed. After four cycles, the furnace was filled with helium to a positive pressure of approximately 5 psi. Next, the furnace was heated at this pressure to the desired temperature, held for the selected soak duration, then allowed to cool.

X-ray diffraction was used to analyze the crystallinity of the carbonized PBO fibers. A 1-in. length of fiber was cemented to a circular aluminum ring. Then, this ring was placed in a Scintag XDS 2000 diffractometer, and Bragg scans were performed to determine the average interplanar (d_{002}) spacing and the average stack height (L_c) of the graphene layer planes.[12] A Split–Pearson VII curve fit was used to deconvolute the diffraction peaks.

RESULTS AND DISCUSSION

Carbonization Kinetics

Mass spectrometry indicated that PBO fibers experience the simultaneous loss of gaseous fragments of diverse molecular weights, as shown in Figure 3. This is consistent with the thermal initiation of free radicals.[13] Figure 4 shows the results of a typical isothermal TGA experiment. The Arrhenius regres-

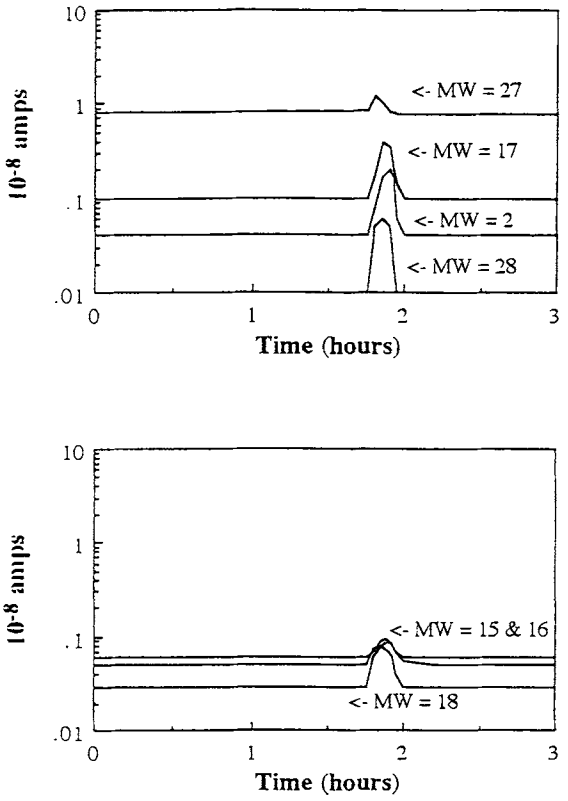

Figure 3 Mass-spectrometric cracking pattern for PBO fiber.

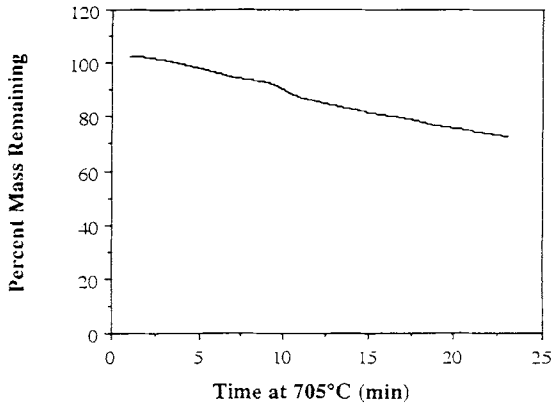

Figure 4 Isothermal TGA of PBO in argon at 705°C.

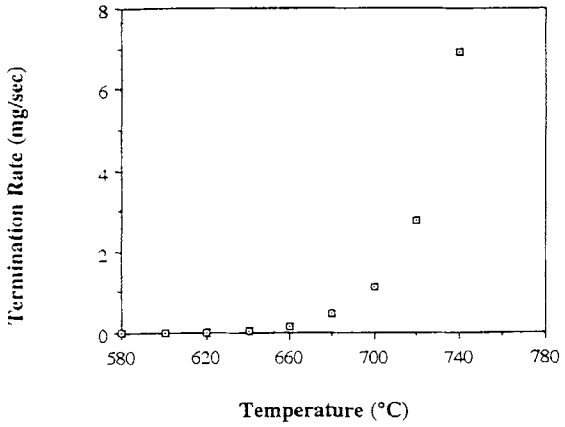

Figure 6 Effect of temperature on termination rate.

sion of the isothermal TGA data obtained from several different temperatures, ranging between approximately 650 and 780°C, is shown in Figure 5. The regression determined an activation energy of 76 ± 6 kcal/mol for the free-radical initiation. To verify that the carbonization process was not diffusion limited, the same experiment described above was repeated in carbon dioxide. Because carbon dioxide is a major product of the carbonization reaction, the results of the TGA should be significantly different in a CO_2 atmosphere, if the process was diffusion limited. No significant variation was observed between trials run in argon and carbon dioxide.

The isothermal result can be used to estimate the general behavior of the termination rate at different temperatures of a ramped TGA trial as described in the Theoretical section. Figure 6 shows how the termination rate varies with temperature. As one might expect, the termination rate was insignificant at low temperatures, but became increasingly important as temperature increased. This supports the fundamental assumption of this model. Figure 6 also indicates that data obtained from isothermal trials can be applied to ramped trials. The combined results of these experiments then can be used to estimate an effective termination rate.

This analysis is not intended as a definitive molecular mechanism for the carbonization of PBO fibers. Instead, this technique demonstrated that the carbonization of PBO fibers can be modeled as a free-radical polymerization and relevant kinetic parameters can be determined. Additionally, some preliminary insight into the nature of the chemical changes occurring in PBO fibers during carbonization can be gained. Specifically, the relative rate of carbonization, a potential model for the reactions, and the identity decomposition products have been determined.

Graphitization Kinetics

Figure 7 shows that carbonized PBO fibers become increasingly ordered with elevated treatment tem-

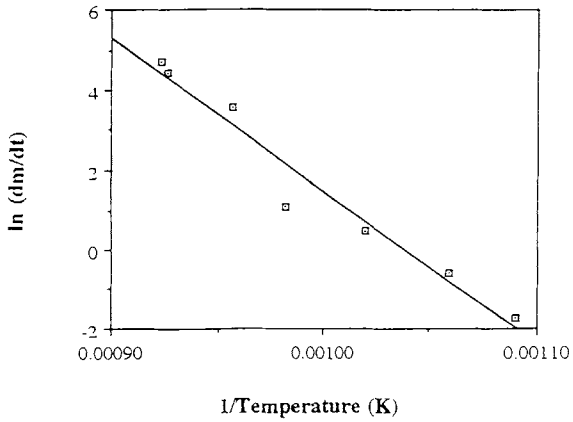

Figure 5 Arrhenius regression of carbonization data.

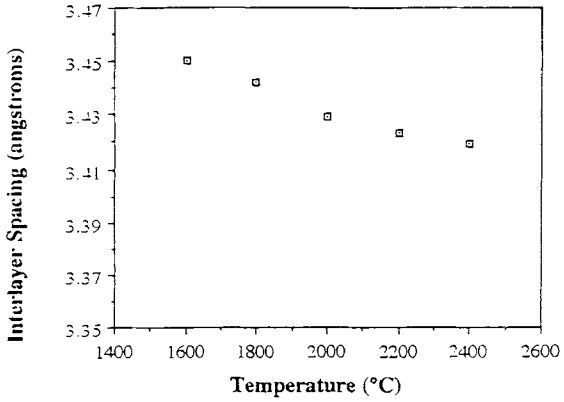

Figure 7 Influence of treatment temperature on interlayer spacing for samples with a 15-min soak duration.

Table II Electrical Resistivities of Carbon Fibers from Various Precursors

Fiber Type	Precursor	Electrical Resistivity ($\mu\Omega$ m)
T-300[a]	PAN	18.0
T-650[a]	PAN	14.9
T-40[a]	PAN	14.5
P-25[a]	Pitch	13.0
PBO-1400°C	PBO	11.0
P-55[a]	Pitch	8.5
P-75[a]	Pitch	7.0

[a] From Thornel.[19]

peratures. The first signs of long-range order appear at 1600°C, where the average interlayer spacing is nearly 3.45 Å for fibers left at that temperature for 15 min. The fiber develops more order as temperatures rise, finally achieving an interlayer spacing of 3.42 Å at 2400°C. Clearly, carbonized PBO does not approach the 3.35-Å interlayer spacing associated with crystalline graphite. However, PBO does develop more order than fibers made from other more common polymeric carbon fiber precursors such as PAN. It may be this order that enables PBO-based carbon fibers to develop electrical resistivities lower than commercial PAN-based fibers, as shown in Table II.[19] The exact mechanism that enables PBO to develop this order is not clear. However, it is probable that the extreme order of the PBO polymer facilitates nucleation, and thus, crystallite growth.

The interlayer spacing of the fibers continues to decrease as the exposure to elevated temperatures increases. Figure 8 shows that the interlayer spacing of PBO-based carbon fibers decreases with increased soak duration. In fact, PBO-based fibers held at

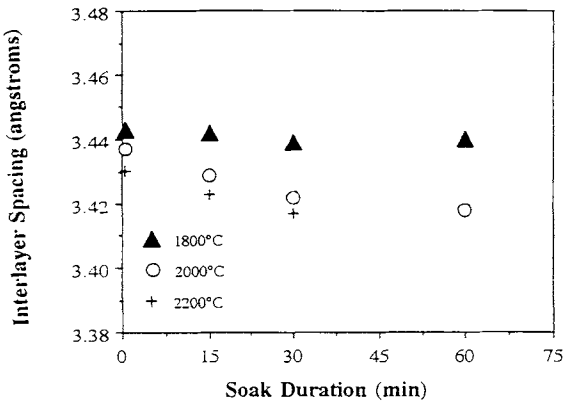

Figure 8 Influence of soak duration on interlayer spacing.

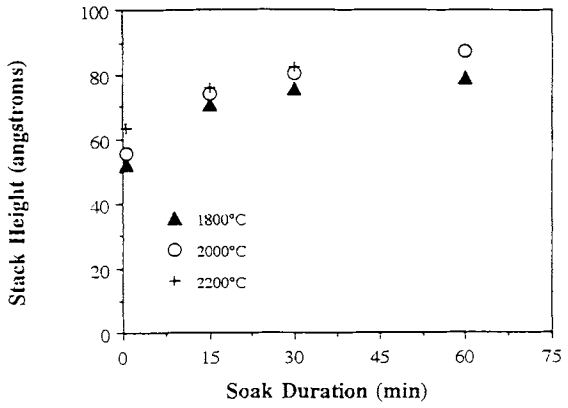

Figure 9 Influence of soak duration on stack height.

2200°C for 30 min have the same interlayer spacing as fibers exposed to 2400°C for a few seconds.

Figure 9 shows that the crystallite size also increases with the duration of the high temperature soak. The data presented in Figure 9 were used to determine an average dL_c/dt for each treatment temperature. The averages were applied to eq. (9). The resultant linear least squares regression on these data provided an estimate for the activation energy of 120 ± 17 kcal/mol. Typical activation energies for the graphitization of other precursor materials have been reported to range from 100 to 250 kcal/mol.[1,17,20] Therefore, the graphitization kinetics and behavior of PBO-based fibers appear to be similar to that of other common carbon fiber precursors.

CONCLUSIONS

This article presents the first study of the graphitization behavior and the carbonization kinetics of PBO fiber. Unlike most polymeric-based fibers, the unique molecular structure of PBO enables the unstabilized fiber to develop some long-range order. An activation energy of 120 ± 17 kcal/mol was determined for the crystallite growth associated with graphitization. This order enables PBO-based fibers to achieve excellent lattice-based properties. The electrical resistivity of PBO-based fibers is superior to that of most commercial PAN-based fibers and is in the range of some commercial pitch-based fibers. Finally, this study showed that the carbonization of PBO could be modeled as a free-radical polymerization. An activation energy of 76 ± 6 kcal/mol was determined for the thermal initiation of radicals. This is comparable to the activation energy range for petroleum pitch feed stocks, which are reported to vary between 43 and 98 kcal/mol.[21] Al-

though the activation energy of PBO is relatively high, this is expected for a material with its thermal stability.

REFERENCES

1. E. Fitzer, *Carbon,* **27**(5), 621 (1989).
2. R. J. Young, R. J. Day, and M. Zakahani, *J. Mater. Sci.,* **25,** 127 (1990).
3. S. Kumar, in *Encyclopedia of Composites,* VCH Publishers, New York, 1990.
4. S. Kumar and T. E. Helminiak, *SAMPE J.,* **26**(2), 51 (1990).
5. I. M. Kowalsky, in *32nd Annual SAMPE Symposium,* Anaheim, CA, April 1987, p. 953.
6. J. G. Glatz, M. A. Kinna, and W. C. Riley, *DOD Metal Matrix Compos. Anal. Center, Curr. Highlights,* **8,** 1 (1988).
7. J. A. Newell, D. K. Rogers, D. D. Edie, and C. C. Fain, *Carbon,* **32**(4), 651 (1994).
8. J. A. Newell and D. D. Edie, *Carbon,* to appear.
9. I. C. Lewis, *Carbon,* **18,** 191 (1980).
10. I. C. Lewis and B. A. Petro, *J. Polym. Sci., Polym. Chem. Ed.,* **14,** 1975 (1976).
11. H. Honda, H. Kimura, Y. Sanada, S. Sugawara, and T. Furata, *Carbon,* **8,** 181 (1970).
12. W. Ruland, *Carbon,* **2,** 365 (1965).
13. L. S. Singer and I. C. Lewis, *Carbon,* **16,** 417 (1978).
14. S. Mrozowski, in *Kinetics of High-Temperature Processes,* W. D. Kingery, Ed., Wiley, New York, 1958.
15. J. K. Kochi, *Free Radicals,* Wiley, New York, 1973.
16. A. M. North, *The Kinetics of Free-Radical Polymerization,* Pergamon Press, New York, 1966.
17. E. Fitzer and S. Weisenberg, *Carbon,* **14,** 323 (1976).
18. H. L. Ledbetter, S. Rosenburg, and C. W. Hurtig, *Mater. Res. Soc. Proc.,* **34,** 253 (1989).
19. *Thornel Product Information,* Amoco Performance Products, Inc., Atlanta, GA, 1991.
20. D. B. Fischbach, *Chem. Phys. Carbon,* **7,** 1 (1971).
21. B. A. Newman, in *Carbon '86* [Extended Abstracts and Program], Pergamon, New York, 1986, p. 147.

Received July 7, 1995
Accepted October 13, 1995